

# Experimental hints on the high-density symmetry energy

Gao-Chan Yong

*Institute of Modern Physics, Chinese Academy of Sciences, Lanzhou 730000, China*

## Abstract

By considering both the effects of the nucleon-nucleon short-rang correlations and the isospin-dependent in-medium inelastic baryon-baryon scattering cross section in the transport model, two experimental measurements at 400 MeV/nucleon beam energy are simultaneously analyzed, a mildly soft symmetry energy at super-saturation densities is obtained.

PACS numbers: 25.70.-z, 21.65.Cd, 21.65.Mn, 21.65.Ef

## I. INTRODUCTION

The nuclear symmetry energy describes the single nucleonic energy of nuclei or nuclear matter changes as one replaces protons in a system with neutrons. Besides its impacts in nuclear physics [1, 2], in a density range of  $0.1 \sim 10$  times nuclear saturation density, the symmetry energy determines the birth of neutron stars and supernova neutrinos [3], a range of neutron star properties such as cooling rates, the thickness of the crust, the mass-radius relationship, and the moment of inertia [4–7]. The nuclear symmetry energy also plays crucial role in the evolution of core-collapse supernovae [8] and astrophysical r-process nucleosynthesis [9]. Thus the better we can constrain the symmetry energy in laboratory measurements, the more we can learn from astroobservations.

To constrain the symmetry energy in broad density regions, besides the studies in astrophysics [10, 11], many terrestrial experiments are still being carried out or planned using a wide variety of advanced new facilities, such as the Facility for Rare Isotope Beams (FRIB) in the US, or the Radioactive Isotope Beam Facility (RIBF) in Japan. To unscramble symmetry energy related experimental data, various isospin-dependent transport models are frequently used to probe the symmetry energy below and above saturation density [1, 2]. With great efforts, the nuclear symmetry energy and its slope around saturation density of nuclear matter from 28 analysis of terrestrial nuclear laboratory experiments and astrophysical observations have been roughly pinned down [12], while recent interpretations of the FOPI and FOPI-LAND experimental measurements by different groups made the symmetry energy at super-saturation densities fall into chaos [13].

Recently, the high-momentum transfer measurements showed that nucleons in nucleus can form pairs with large relative momenta and small center-of-mass momenta [14, 15]. This phenomenon was explained by the short-rang nucleon-nucleon tensor interaction [16, 17]. Such nucleon-nucleon short-range correlations (SRC) in nucleus leads to a high-momentum tail (HMT) in the single-nucleon momentum distribution [18–20, 31]. More interestingly, in the HMT of nucleon momentum distribution, nucleon component is evidently isospin-dependent. The number of n-p SRC pairs are about 18 times that of the p-p and n-n SRC pairs [22]. And in neutron-rich nucleus, proton has a greater probability than neutron to have momentum greater than the nuclear Fermi momentum [23].

Unfortunately, effects of the above isospin-dependent SRC was seldom taken into ac-

count in most of currently used isospin-dependent transport models, while the latters have been frequently used to unscramble symmetry energy related experimental data [24–29]. To extract information of the symmetry energy from experimental data, in this study, by considering both the effects of the isospin-dependent SRC and the important but often-overlooked in-medium baryon-baryon inelastic cross section in the isospin-dependent transport model, unrelated experimental measurements are simultaneously analyzed.

## II. THE IBUU TRANSPORT MODEL

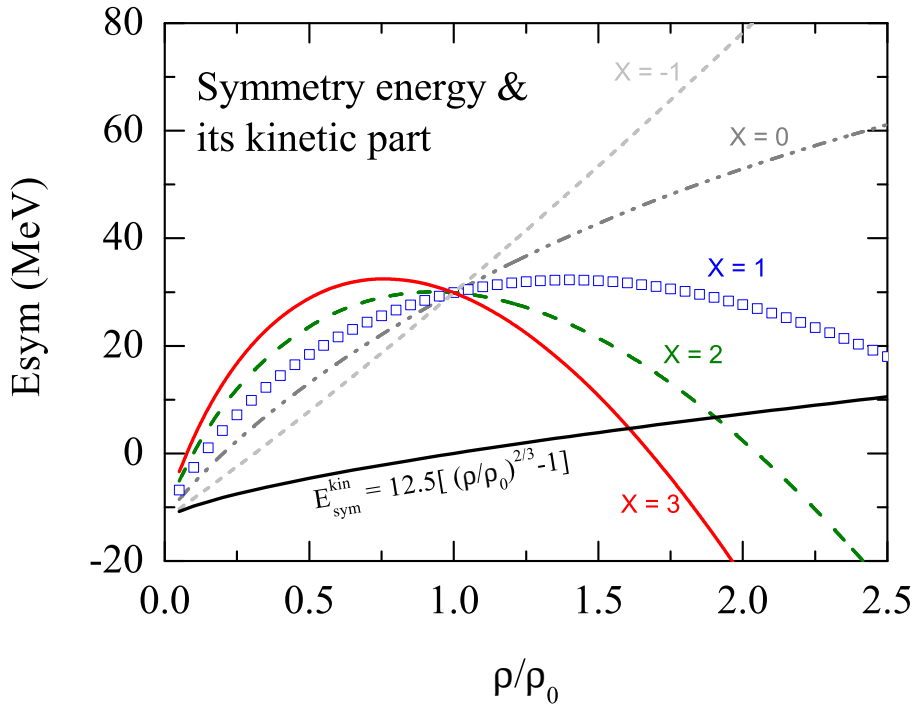


FIG. 1: (Color online) Kinetic symmetry energy and density-dependent symmetry energy with different  $x$  parameters. Note here that in heavy-ion collisions at 400 MeV/nucleon beam energy, the high-density part of the symmetry energy plays major role.

To probe the symmetry energy from experimental data, We use our recent updated Isospin-dependent Boltzmann-Uehling-Uhlenbeck (IBUU) transport model [30]. In this

IBUU model, nucleon-density distribution is given by

$$\begin{aligned} r &= R(x_1)^{1/3}; \cos\theta = 1 - 2x_2; \phi = 2\pi x_3; \\ x &= r\sin\theta\cos\phi; y = r\sin\theta\sin\phi; z = r\cos\theta. \end{aligned} \quad (1)$$

Where  $R$  is the radius of nucleus,  $x_1, x_2, x_3$  are three independent random numbers. Since there is a depletion of nucleon distribution inside the Fermi sea, the proton and neutron momentum distributions with high-momentum tail at about 2 times the Fermi momentum [30] are given by the extended Brueckner-Hartree-Fock (BHF) approach by adopting the AV 18 two-body interaction plus a microscopic Three-Body-Force (TBF) [31]. Compared with the distribution in ideal Fermi gas, the excess average kinetic energy of nucleon in colliding nuclei is subtracted from the total energy of reaction system.

In this model, an isospin- and momentum-dependent mean-field single nucleon potential is used, i.e.,

$$\begin{aligned} U(\rho, \delta, \vec{p}, \tau) &= A_u(x) \frac{\rho_{\tau'}}{\rho_0} + A_l(x) \frac{\rho_{\tau}}{\rho_0} \\ &+ B \left( \frac{\rho}{\rho_0} \right)^{\sigma} (1 - x\delta^2) - 8x\tau \frac{B}{\sigma + 1} \frac{\rho^{\sigma-1}}{\rho_0^{\sigma}} \delta \rho_{\tau'} \\ &+ \frac{2C_{\tau,\tau}}{\rho_0} \int d^3 \vec{p} \frac{f_{\tau}(\vec{r}, \vec{p}')}{1 + (\vec{p} - \vec{p}')^2 / \Lambda^2} \\ &+ \frac{2C_{\tau,\tau'}}{\rho_0} \int d^3 \vec{p} \frac{f_{\tau'}(\vec{r}, \vec{p}')}{1 + (\vec{p} - \vec{p}')^2 / \Lambda^2}, \end{aligned} \quad (2)$$

where  $\tau, \tau' = 1/2(-1/2)$  for neutrons (protons),  $\delta = (\rho_n - \rho_p)/(\rho_n + \rho_p)$  is the isospin asymmetry, and  $\rho_n, \rho_p$  denote neutron and proton densities, respectively. Parameter settings can be found in Ref. [30], Different symmetry energy's stiffness parameter  $x$  can be used in the above single nucleon potential to mimic different forms of the symmetry energy. Since the kinetic symmetry energy, even its sign, is still controversial [32], we at present give it a null value [33]. For its density-dependence, we use similar form as that from the ideal Fermi gas model. Thus the density-dependent kinetic symmetry energy is as following

$$E_{sym}^{kin} = 12.5[(\rho/\rho_0)^{2/3} - 1]. \quad (3)$$

Fig. 1 shows the kinetic symmetry energy we used and the density-dependent symmetry energy with different  $x$  parameters. It is seen that our used density-dependent kinetic

symmetry energy is similar to that in Ref. [32, 34]. We can also see that  $x = 1, 0, -1$  cases roughly correspond positive slope ( $L(\rho_0) \equiv 3\rho_0 dE_{sym}(\rho)/d\rho$ ) 37, 87, 138 MeV, respectively. The isospin-dependent baryon-baryon ( $BB$ ) scattering cross section (elastic or inelastic) in medium  $\sigma_{BB}^{medium}$  is reduced compared with their free-space value  $\sigma_{BB}^{free}$  by a factor of

$$R_{medium}(\rho, \delta, \vec{p}) \equiv \sigma_{BB_{elastic}}^{medium} / \sigma_{BB_{elastic}}^{free} = (\mu_{BB}^* / \mu_{BB})^2, \quad (4)$$

where  $\mu_{BB}$  and  $\mu_{BB}^*$  are the reduced masses of the colliding baryon-pair in free space and medium, respectively. More details can be found in Ref. [30].

### III. RESULTS AND DISCUSSIONS

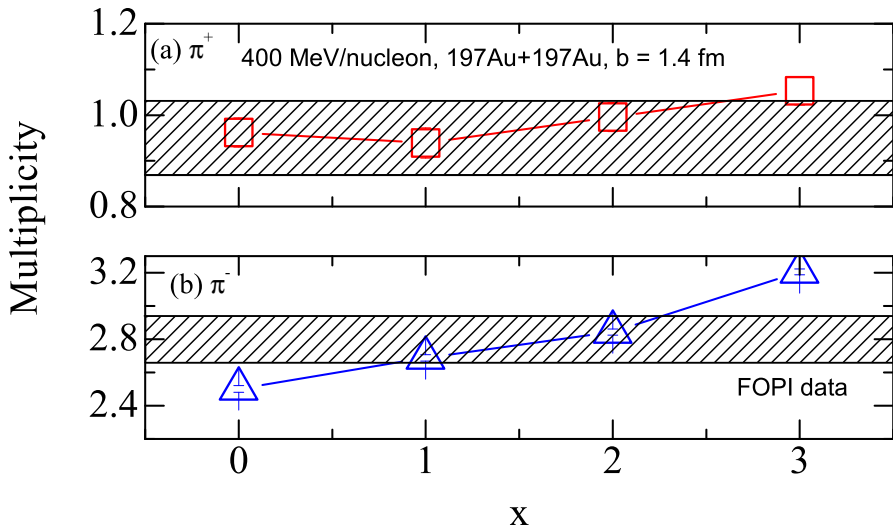


FIG. 2: (Color online) Multiplicity of charged pion meson produced in Au+Au reaction at 400 MeV/nucleon with different symmetry energies. The shadow region denotes the FOPI data [35].

Before studying the  $\pi^-/\pi^+$  ratio, it is instructive to first see the production of charged pion meson in central Au + Au reaction at 400 MeV/nucleon beam energy. Fig. 2 shows numbers of charged pion produced with different symmetry energies. It is seen that both produced  $\pi^-$  and  $\pi^+$  fit the FOPI experimental data quite well. With stiffer symmetry

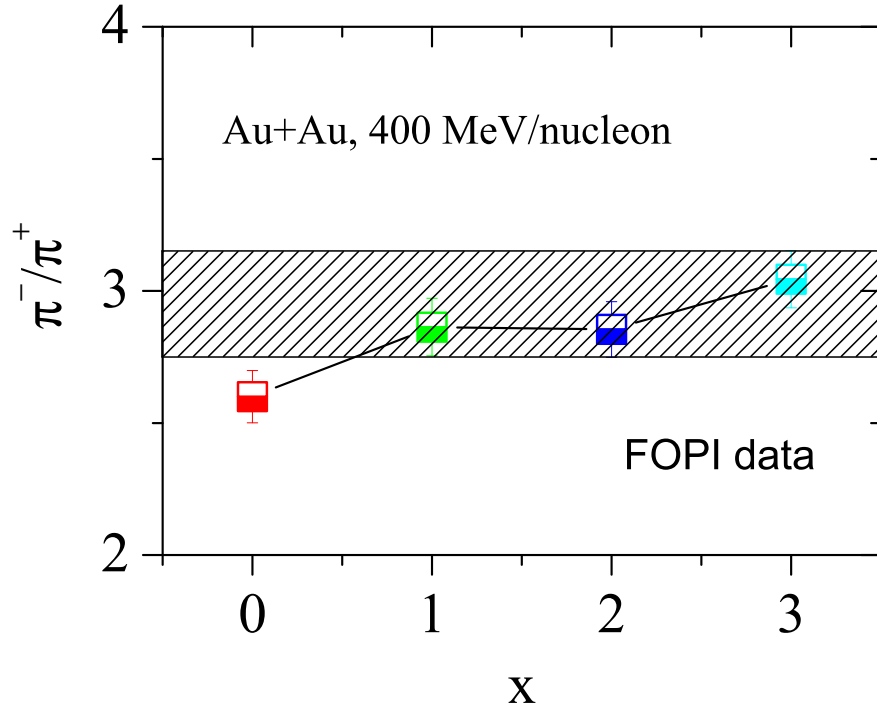


FIG. 3: (Color online)  $\pi^-/\pi^+$  ratio in Au+Au reaction at 400 MeV/nucleon with different symmetry energies.

energy  $x = 0$ , the model gives somewhat smaller  $\pi^-$  number than experimental data. While with very soft symmetry energy  $x = 3$ , the model gives both larger  $\pi^+$  and  $\pi^-$  numbers than experimental data. Comparing upper panel with lower panel, it is seen that sensitivity of the number of produced  $\pi^-$  to the symmetry energy is at least 3 times that of  $\pi^+$ . Fig. 2 shows the  $\pi^-/\pi^+$  ratio predicted by our IBUU model with different symmetry energies. Because softer symmetry energy causes more neutron-rich dense matter and  $\pi^-$ 's are mainly from neutron-neutron collision whereas  $\pi^+$ 's are mainly from proton-proton collision [36], it is not surprising that one sees larger  $\pi^-/\pi^+$  ratio with softer symmetry energy. From Fig. 3, we can see that the FOPI pion experimental data hints a softer symmetry energy ( $x = 1, 2$ , or even 3).

To further constrain the symmetry energy over a broad region ( $x = 1, 2$ , or even 3) as shown in Fig. 1, one has to search for other constraints. Fig. 4 shows predicted neutron and proton elliptic flows in Au + Au reaction under the FOPI-LAND experimental conditions

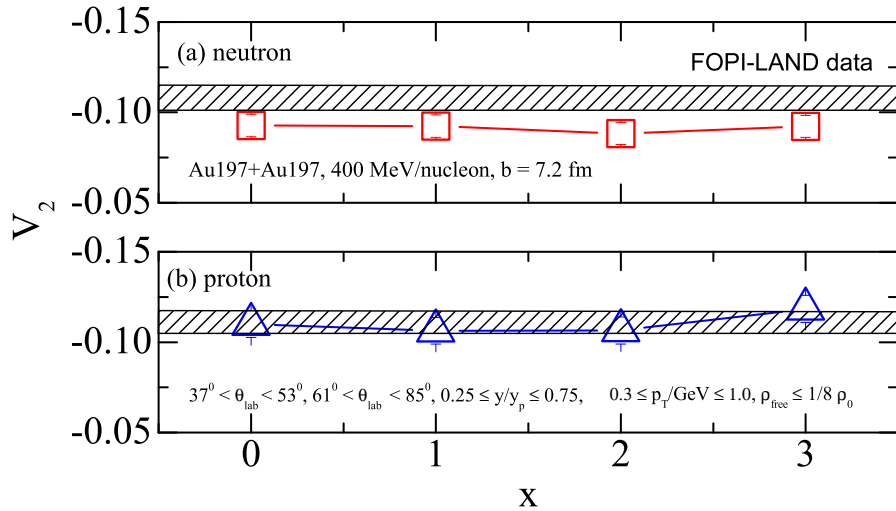


FIG. 4: (Color online) Elliptic flow of emitting nucleon in Au+Au collision at 400 MeV per nucleon incident beam energy with different symmetry energies. The shadow region denotes the experimental FOPI-LAND data [28].

and geometry [28]. The experimental data is multiplied with a factor 1.15 due to dispersion of the reaction plane [37]. From Fig. 4 (a), it is seen that our model give lower value of the elliptic flow of neutron. However, from Fig. 4 (b), it is seen that the predicted elliptic flow of proton fit experimental quite well. In our model, free nucleons are identify by its local density  $\rho_{free} \leq \rho_0/8$ , the latter is the deuteron density  $0.02 \text{ fm}^{-3}$ . From Fig. 4, we can see that both proton and neutron elliptic flows are in fact not sensitive to the symmetry energy at such experimental conditions and geometry. Shown in Fig. 5 is predicted elliptic flow ratios of neutron and proton  $V_2^n/V_2^p$  with different symmetry energies as well as experimental data [28]. Since stiffer symmetry energy causes more squeezed-out neutrons to emit in the direction perpendicular to the reaction plane [38], one sees larger values of elliptic flow ratios of neutron and proton  $V_2^n/V_2^p$  with stiffer symmetry energies. This figure indicates the FOPI-LAND elliptic flow experimental data does not favor very soft symmetry energy ( $x = 2, 3$ ).

Combining the studies of nucleon elliptic flow and previous  $\pi^-/\pi^+$ , one can roughly obtain the symmetry energy stiffness parameter  $x = 1$ . It in fact corresponds a mildly soft density-

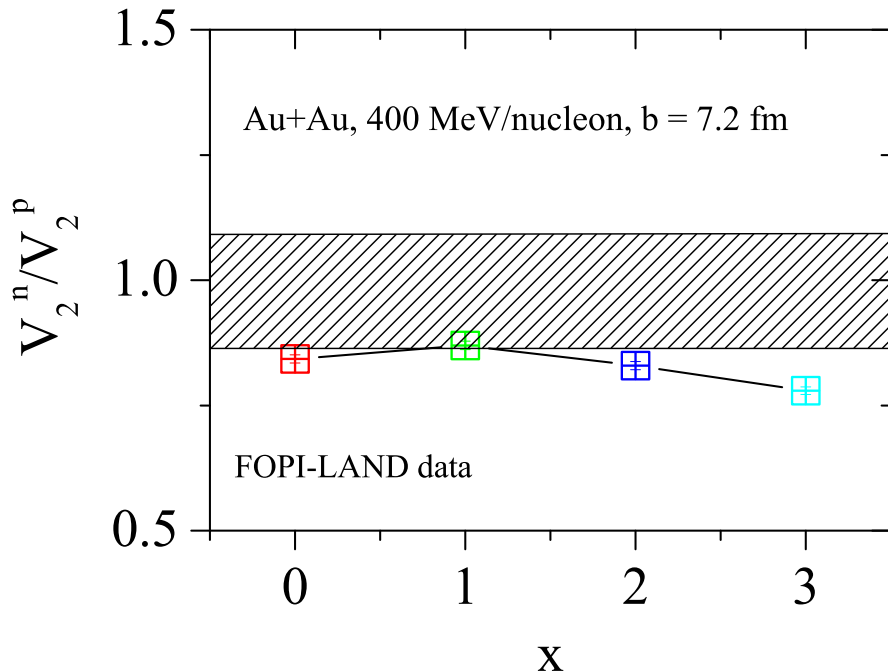


FIG. 5: (Color online) Same as Fig. 4, but for the ratio of  $V_2^n/V_2^p$ .

dependent symmetry energy at super-saturation densities. While the specific density region of the present constraints on the nuclear symmetry energy needs to be further studied [42].

#### IV. CONCLUSIONS

Using the FOPI and FOPI-LAND experimental measurements, based on the newly updated transport model, the symmetry energy at super-saturation densities is roughly constrained. The study indicates a mildly soft density-dependent symmetry energy at super-saturation densities. Since the nuclear symmetry energy plays crucial roles in both nuclear physics and astrophysics, more related experimental and theoretical efforts are still needed to pin down the symmetry energy at super-saturation densities.

## Acknowledgements

The author thanks M. D. Cozma for providing the FOPI-LAND elliptic flow analysis routine and helpful discussions. The work was carried out at National Supercomputer Center in Tianjin, and the calculations were performed on TianHe-1A. The work is supported by the National Natural Science Foundation of China under Grant Nos. 11375239, 11435014.

---

- [1] V. Baran, M. Colonna, V. Greco, M. Di Toro, *Phys. Rep.* **410**, 335 (2005).
- [2] B. A. Li, L. W. Chen and C. M. Ko, *Phys. Rep.* **464**, 113 (2008).
- [3] K. Sumiyoshi, H. Suzuki, H. Toki, *Astron. Astrophys.* **303**, 475 (1995).
- [4] K. Sumiyoshi and H. Toki, *Astrophys. J.* **422**, 700 (1994).
- [5] J. M. Lattimer, M. Prakash, *Science* **304**, 536 (2004).
- [6] A. W. Steiner, M. Prakash, J. M. Lattimer, P. J. Ellis, *Phys. Rep.* **411**, 325 (2005).
- [7] James M. Lattimer, Andrew W. Steiner, *Eur. Phys. J. A* **50**, 40 (2014).
- [8] T. Fischer et al., *Eur. Phys. J. A* **50**, 46 (2014).
- [9] N. Nikolov, N. Schunck, W. Nazarewicz, M. Bender, and J. Pei, *Phys. Rev. C* **83**, 034305 (2011).
- [10] F. J. Fattoyev, J. Carvajal, W. G. Newton, Bao-An Li, *Phys. Rev. C* **87**, 015806 (2013).
- [11] F. J. Fattoyev, W. G. Newton, Bao-An Li, *Eur. Phys. J. A*, **50**, 45 (2014).
- [12] B.A. Li, X. Han, *Phys. Lett. B* **727**, 276 (2013).
- [13] W. M. Guo, G. C. Yong, Y. J. Wang, Q. F. Li, H. F. Zhang, W. Zuo, *Phys. Lett. B* **738**, 397 (2014).
- [14] E. Piasetzky, M. Sargsian, L. Frankfurt, M. Strikman, J. W. Watson, *Phys. Rev. Lett.* **97**, 162504 (2006).
- [15] R. Shneor et al., *Phys. Rev. Lett.* **99**, 072501 (2007).
- [16] M. M. Sargsian, T. V. Abrahamyan, M. I. Strikman and L. L. Frankfurt, *Phys. Rev. C* **71**, 044615 (2005).
- [17] R. Schiavilla, R. B. Wiringa, S. C. Pieper and J. Carlson, *Phys. Rev. Lett.* **98**, 132501 (2007).
- [18] H. A. Bethe, *Ann. Rev. Nucl. Part. Sci.* **21**, 93 (1971).
- [19] A. N. Antonov, P. E. Hodgson and I. Z. Petkov, *Nucleon Momentum and Density Distributions*

*in Nuclei* (Clarendon Press, Oxford, 1988).

- [20] A. Rios, A. Polls, and W. H. Dickhoff, Phys. Rev. C **79**, 064308 (2009).
- [21] P. Yin, J. Y. Li, P. Wang, and W. Zuo, Phys. Rev. C **87**, 014314 (2013).
- [22] R. Subedi et al. (Hall A. Collaboration), Science **320**, 1476 (2008).
- [23] O. Hen et al. (The CLAS Collaboration), Science **346**, 614 (2014).
- [24] D. V. Shetty, S. J. Yennello, and G. A. Souliotis, Phys. Rev. C **76**, 024606 (2007).
- [25] M. B. Tsang et al., Phys. Rev. Lett. **102**, 122701 (2009).
- [26] W. G. Lynch et al., Prog. Part. Nucl. Phys. **62**, 427 (2009).
- [27] Z. G. Xiao, B. A. Li, L. W. Chen, G. C. Yong, M. Zhang, Phys. Rev. Lett. **102**, 062502 (2009).
- [28] M. D. Cozma, Y. Leifels, W. Trautmann, Q. Li, P. Russotto, Phys. Rev. C **88**, 044912 (2013).
- [29] J. B. Natowitz et al., Phys. Rev. Lett. **104**, 202501 (2010).
- [30] G. C. Yong, arXiv: 1503.08523 (2015).
- [31] P. Yin, J. Y. Li, P. Wang, and W. Zuo, Phys. Rev. C **87**, 014314 (2013).
- [32] O. Hen, B. A. Li, W. J. Guo, L. B. Weinstein, and E. Piasetzky, Phys. Rev. C **91**, 025803 (2015).
- [33] I. Vidana, A. Polls, C. Providencia, Phys. Rev. C **84**, 062801 (R) (2011).
- [34] A. Carbone, A. Polls, and A. Rios, Europhys. Lett. **97**, 22001 (2012).
- [35] W. Reisdorf et al. (FOPI Collaboration), Nucl. Phys. A **848**, 366 (2010).
- [36] B. A. Li, G. C. Yong, W. Zuo, Phys. Rev. C **71**, 014608 (2005).
- [37] M. D. Cozma, private communications
- [38] G. C. Yong, B. A. Li, L. W. Chen, Phys. Lett. B **650**, 344 (2007).
- [39] L. Zhang, Y. Gao, Y. Du, G. H. Zuo, G. C. Yong, Eur. Phys. J. A **48**, 30 (2012).
- [40] W. Reisdorf et al. (FOPI Collaboration), Nucl. Phys. A **781**, 459 (2007).
- [41] B. A. Li, Phys. Rev. C **67**, 017601 (2003).
- [42] H. L. Liu, G. C. Yong, D. H. Wen, Phys. Rev. C **91**, 044609 (2015).